

# Single Crystal Growth of $\text{FeGa}_3$ and $\text{FeGa}_{3-x}\text{Ge}_x$ from High-Temperature Solution Using the Czochralski Method

Kristian Bader and Peter Gille\*

Single crystal growth and characterization of the binary semiconducting compound  $\text{FeGa}_3$  and its Ge-substitute  $\text{FeGa}_{3-x}\text{Ge}_x$  are reported. Whereas there have been several investigations on the thermoelectric properties based on small samples grown by the flux method, this study is the first approach using the Czochralski growth technique from well-oriented single-crystalline seeds. Problems and solutions of the growth of  $\text{cm}^3$ -size single crystals are discussed in detail. Ge segregation in  $\text{FeGa}_{3-x}\text{Ge}_x$  is described by a segregation coefficient lower than unity which leads to an axially increasing Ge content along the pulling direction. Consequences with respect to lattice parameter changes and thermoanalytic measurements are reported.

## 1. Introduction

There are only rare examples of two genuine metals which combine to form a semiconducting compound.  $\text{FeGa}_3$  is one of these and was first described in detail by Häussermann et al.<sup>[1]</sup> It has been found that Fe and Ga strongly interact opening a  $d$ - $p$  hybridization narrow bandgap. Looking into the neighborhood of Fe and Ga in the periodic table of the elements to search for pairs with a similar behavior, it has been established what is called the 17-electrons rule:  $d$ -electron metals from the eighth group with  $p$ -electron metals from the 13th group form narrow-gap semiconductors, for example,  $\text{FeGa}_3$ ,  $\text{RuGa}_3$ , and  $\text{RuIn}_3$ , while, for example,  $\text{CoGa}_3$ ,  $\text{CoIn}_3$ , and  $\text{IrIn}_3$  having 18 valence electrons show metallic conductivity.<sup>[1–3]</sup>

Besides this academic point of view,  $\text{FeGa}_3$  and homologous semiconductors have gained additional interest for thermoelectric applications.<sup>[4–6]</sup> Apart from pure  $\text{FeGa}_3$ , there have been several studies to partially substitute Fe by Ru, Co, Mn, or Ni, or Ga by Al, In, Zn, or Ge to investigate thermoelectric properties and to increase the figure of merit.<sup>[7–17]</sup>

K. Bader, Prof. P. Gille  
Ludwig-Maximilians-Universität München  
Department of Earth and Environmental Sciences  
Crystallography Section  
Theresienstr. 41, D-80333 München, Germany  
E-mail: gille@lmu.de

The ORCID identification number(s) for the author(s) of this article can be found under <https://doi.org/10.1002/crat.201900067>

© 2019 The Authors. Published by WILEY-VCH Verlag GmbH & Co. KGaA, Weinheim. This is an open access article under the terms of the Creative Commons Attribution License, which permits use, distribution and reproduction in any medium, provided the original work is properly cited.

DOI: 10.1002/crat.201900067

Improvements of the thermopower of  $\text{FeGa}_3$  by Ge electron doping revealed important new properties of  $\text{FeGa}_{3-x}\text{Ge}_x$ . Starting from a semiconductor, with increased Ge doping the compound performs a crossover to a strongly correlated metal at  $x = 0.06$ .<sup>[11,18]</sup> Arising from the sensitivity of strongly correlated materials to chemical doping, it was found that at the critical Ge concentration of around  $x = 0.15$ , the phase shows quantum critical fluctuations and a phase transition from antiferromagnetic to itinerant ferromagnetism at low temperatures. While antiferromagnetic quantum critical

systems have already been studied in  $4f$  and  $3d$ -systems, ferromagnetic quantum criticality is of significant interest for basic research.<sup>[19]</sup>

According to these various origins of interest in  $\text{FeGa}_3$  and related intermetallics, there have been several attempts to grow single crystals. Surprisingly, to the best of the authors' knowledge all these crystal growth studies used exclusively a single method which is usually called (self-) flux method tracing back to Fisk's pioneering work.<sup>[20]</sup> This technique has the advantage of a low-cost and easy-to-do approach which often has provided the very first samples of a new phase,<sup>[21]</sup> but it lacks like other black-box methods from missing observation during the growth process. Thus, any influence on the growth process is limited. Nevertheless, a lot of studies of  $\text{FeGa}_3$  and related phases were carried out using single-crystalline samples obtained from the flux method and the largest example of a single crystal obtained by this preparation route has been published by Likhonov et al.<sup>[17]</sup> Even this crystal had only a size of a few mm. Due to spontaneous nucleation, reproducible growth cannot be achieved using the flux method.

Being quite experienced with the Czochralski method of growing intermetallic phases, we tried to apply this technique to  $\text{FeGa}_3$  and  $\text{FeGa}_{3-x}\text{Ge}_x$  in order to allow single crystal growth in a reproducible manner based on a defined crystallographic direction given by oriented native seed crystals.  $\text{FeGa}_3$ , like the related phases mentioned above crystallizes in the space group  $P4_2/mnm$  (no. 136). Detailed crystallographic data were studied by Häussermann et al.<sup>[1]</sup>

## 2. Growth Strategy

### 2.1. Binary $\text{FeGa}_3$ Single Crystal Growth

According to the well-accepted binary phase diagram by Okamoto<sup>[22]</sup> (see Figure 1),  $\text{FeGa}_3$  is a compound that peri-

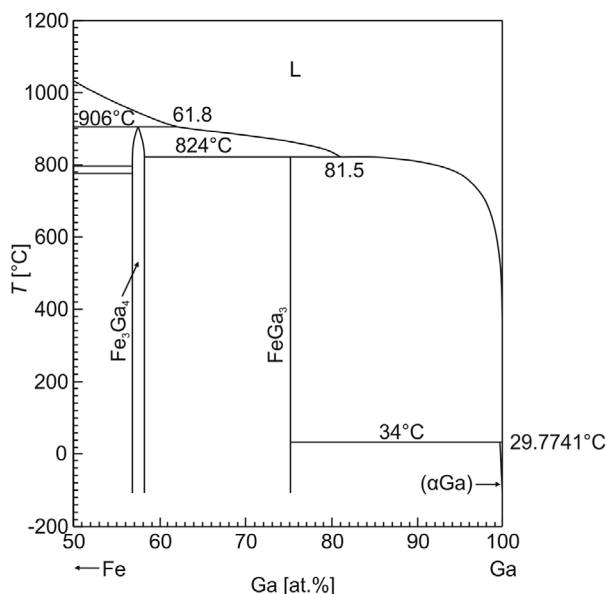


**Figure 1.** Ga-rich part of the Fe-Ga phase diagram, redrawn after Okamoto.<sup>[22]</sup>

tectically decomposes at a temperature of 824 °C and can, therefore, only be grown below its peritectic temperature, that is, from a Ga-rich solution with at least 81.5 at% Ga. Due to an extremely shallow, almost horizontal slope of the liquidus line next to the peritectic point, the Fe content in the solution quickly decreases to less than 1 at% solubility at a temperature of approx. 600 °C which is considered—for practical purposes—the very end of any growth process. These limits arising from thermodynamics are the same with any other crystal growth technique from a binary solution as well, for example, with the flux method. Among all possible methods the authors of the present paper regard the Czochralski technique to be the best suited one, mainly because of good observation during the whole growth process.

One of the additional advantages of Czochralski growth is the relatively easy seeding procedure. But, when starting an experiment with a new phase, there is often no native seed available which is large enough to be mounted at the seed holder. In literature, there have been several suggestions how to get the very first crystalline material from a new phase by spontaneous nucleation onto a suitable other material.<sup>[23–25]</sup> In order to achieve nucleation of the FeGa<sub>3</sub> phase we decided to use a tapered alumina rod mounted at the end of the pulling axis. Coming from a colder environment, the tip of the alumina rod would act as a cold point making the tip an exclusive site for nucleation when brought into contact with a slightly undercooled solution. From such a first experiment, one cannot be sure to get a single crystal or even a well oriented one. But, from the authors' experience with other phases there has been some hope to grow an ingot large enough to enable the preparation of a single-crystalline seed for a next growth run.

## 2.2. FeGa<sub>3–x</sub>Ge<sub>x</sub> Single Crystal Growth

Growth of FeGa<sub>3–x</sub>Ge<sub>x</sub> single crystals was intended to be the second step of the present project and could be based on the re-

sults obtained with the binary compound. In literature, there has been no ternary Fe-Ga-Ge phase diagram available. Neither the influence of Ge doping on the lattice parameter of FeGa<sub>3</sub> was known. But, due to the similar atomic radii of Ga and Ge we assumed a weak enough lattice parameter change allowing for native seeding with binary FeGa<sub>3</sub> even when trying to grow the ternary FeGa<sub>3–x</sub>Ge<sub>x</sub> solid solution.

Due to the relatively high preparative effort that is necessary to conduct a Czochralski growth experiment, we decided to carry out pre-experiments to study the Ge segregation behavior, that is, to get the Ge concentration,  $x_S$ , being incorporated into the crystal from a Ga-rich solution of known Ge content,  $x_L$ . These simple directional solidification pre-experiments can be done in fused silica ampoules using only small amounts of material and give information about the first-to-freeze composition which results from a known starting charge. Neglecting possible supercooling effects, these two compositions may be regarded as the two compositions being in thermodynamic equilibrium.

Knowing this correlation, it could be decided about the starting composition of the melt for a Czochralski experiment aimed at a specific composition  $x$  of the FeGa<sub>3–x</sub>Ge<sub>x</sub> single crystal. In all cases, the synthesis of the starting elements could be done ex situ in a RF-heated apparatus to be sure to start crystal growth from well-mixed solutions.

## 3. Experimental Section

### 3.1. Synthesis of Binary and Ternary Solutions

Ga-rich binary and ternary starting charges were synthesized only from bulky pieces of the elements in order to avoid large specific surfaces. Parts from iron rods (4N5-grade, ChemPur) were wet-chemically etched using diluted nitric and hydrochloric acids, and germanium pieces (5N-grade, ChemPur) were weighed untreated. Gallium pieces (6N-grade, ChemPur) were reduced in 5N-grade hydrogen atmosphere in a glassy carbon crucible to remove the Ga<sub>2</sub>O<sub>3</sub> surface layer. Typical charges of a total mass of ≈50 g were prepared with an accuracy of at least 0.02 at. %. The starting elements were synthesized using RF-heating in a 10 mL alumina crucible (Alsint 99.7, Haldenwanger) under Ar atmosphere (5N-grade) of ambient pressure after carefully evacuating in a fully metal-sealed vacuum system. Slow heating allows Fe (and Ge) to become dissolved in the Ga-rich solution without approaching the individual melting temperatures. After reaching the maximum temperature of ≈950 °C, the melt was kept for an additional hour at constant temperature in order to complete dissolution and homogenization. Quenching to room temperature was done simply by switching off the RF power. The solidified starting charges could easily be removed from the alumina crucible and were transferred without any further treatment into the growth crucible. Even short-time storage was done under vacuum.

### 3.2. FeGa<sub>3–x</sub>Ge<sub>x</sub> Pre-Experiments

In order to get some preliminary data about the Ge segregation, that is, about the necessary Ge concentration in the starting melt for a target Ge substitution for Ga, simple Bridgman-type normal

freezing experiments were carried out. The syntheses of these starting melts were done in the same way as described above but in tubular alumina crucibles (Alsint 99.7, Haldenwanger) of 10 mm inner diameter. After synthesis, homogenization and quenching in the RF furnace, these crucibles were fused in a silica ampoule after having been filled with Ar atmosphere in order to result in ambient pressure at operation conditions. In a vertical single-zone Bridgman furnace, each ampoule was held at a temperature exceeding 850 °C for about two days to again allow homogenization of the melt and then lowered through a temperature gradient of approx. 10 K cm<sup>-1</sup> using a translation rate of 6 mm d<sup>-1</sup>.

### 3.3. FeGa<sub>3</sub> and FeGa<sub>3-x</sub>Ge<sub>x</sub> Czochralski Experiments

The pre-synthesized binary or ternary charges with compositions of 81.15 to 83.65 at% Ga were again stored in a 10 mL alumina crucible and built into the fully metal-sealed Czochralski apparatus which has been described in a former paper in detail.<sup>[23]</sup> Spontaneous nucleation onto a “cold” ceramic tip was used in the very first FeGa<sub>3</sub> Czochralski growth, but in all subsequent growth runs, a [001]-oriented FeGa<sub>3</sub> seed crystal was prepared from a FeGa<sub>3</sub> single crystal of a former experiment. The 9 mm long wedge-shaped seed was mounted to a ceramic seed holder made from alumina (see Figure 2).

The Czochralski growth chamber was evacuated to a residual pressure of less than 10<sup>-6</sup> mbar and filled with 5N-grade Ar of 550 mbar which resulted in approx. ambient pressure conditions upon heating to growth temperatures. Melting of the starting charge was done using a heating rate of 500 K h<sup>-1</sup> to a target set-

point temperature of 900 °C. In order to assist re-homogenization of the molten material, accelerated crucible rotation (ACRT)<sup>[26]</sup> was used for 18 h. Prior to seeding, the temperature of the melt has to approach its liquidus temperature as close as possible. Since the control thermocouple is not inserted into the melt but in thermal contact to the resistance heater, there is always a difference between the indicated and the actual melt temperature. The exact liquidus temperature condition was found by careful observation of first nucleation at the melt surface during slow cooling followed by very slow heating and recording the temperature when the last crystallites disappeared. After having found these appropriate seeding conditions, a short superheating by 50 K was applied to ensure that all other crystallites were dissolved. Lowering the tip of the seed crystal to the shiny surface of the melt, wetting of the seed crystal suddenly occurred at first touch. Already during the seeding procedure, a slow-speed counter-rotation of the seed and the crucible was used. Again, careful observation of the seed/melt region enabled fine-tuning of the temperature in order to get a close to steady-state situation. Once having found the starting temperature conditions, crystal growth was initiated by pulling the seed upward with a pulling rate of 0.1 mm h<sup>-1</sup>. Crystal rotation was set to 60 rpm and crucible counter-rotation at a rate of 40 rpm. Rotation rates were not changed during the whole growth process, but the pulling rate was gradually reduced to 0.025 mm h<sup>-1</sup>. A progressively decreasing temperature was programmed in order to balance the change of the liquidus temperature due to proceeding crystallization. Since the used Czochralski puller is not equipped with an automatic diameter control, time-to-time observation of the actual diameter determines the change in the temperature program used. While starting with a cooling rate of 0.01 K h<sup>-1</sup>, at the end of the growth runs a rate of up to 0.20 K h<sup>-1</sup> was necessary to get an acceptable diameter of the crystal. Finally, crystal growth was completed by fast detaching the crystal from the rest of the melt. Cooling the crystal to room temperature was done at a rate of 100 K h<sup>-1</sup>.

### 3.4. Surface Preparation

After X-ray orientation using Laue back-scattering technique, the single crystals were transferred to a wire saw (WS 22, KD UNIPRESS, Poland) and cut into slices of well-defined crystallographic surface orientations, usually of the forms {001} or {100}. Using a 50 µm thick tungsten wire and an 800 mesh boron carbide suspension in glycerol, a minimum surface damage and material loss was achieved during cutting. Final surface preparation was done by mechanical polishing with decreasing diamond grain size down to 0.25 µm followed by a chemo-mechanical polishing step with Syton OP-S (Struers).

### 3.5. Characterization Methods

#### 3.5.1. X-Ray Powder Diffraction

X-ray powder diffraction was conducted on a GE Bragg-Brentano diffractometer (XRD3003 TT) using Cu-K<sub>α1</sub> radiation (λ = 0.15406 nm) at 40 kV and 40 mA and a Ge(111) monochro-

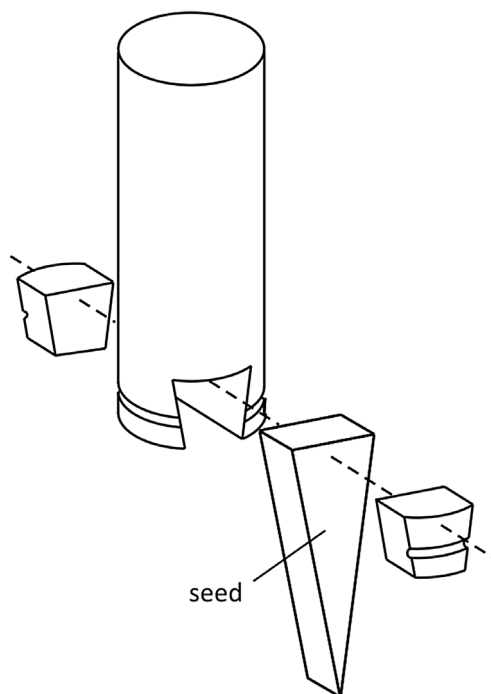


**Figure 2.** Full-ceramic seed holder which fixes a 9 mm long wedge-shaped single-crystalline seed obtained from an earlier experiment. Reproduced with permission.<sup>[23]</sup> Copyright 2008, Wiley-VCH.

mator. On the semiconductor position-sensitive linear detector (Meteor1D) a threshold was set at 7.5 keV to exclude fluorescence of Fe. The powders were placed on a zero-background quartz sample holder at a rotation of 1 Hz and Si640c (NIST) was used as internal standard. Data sets were collected three times in the range of  $2\theta = 10\text{--}120^\circ$  with a step size of  $2\theta = 0.013^\circ$  and added up to improve counting statistics. Refinement of the lattice parameters was performed by LeBail fitting and of the structure by Rietveld using the program package FullProf.<sup>[27]</sup>

### 3.5.2. Laue Backscattering Method

Laue X-ray diffraction in the back-scattering mode was used to test the single-crystallinity of the grown samples by scanning along the axial position of the ingot with the crystal kept in fixed orientation. The Laue technique was also applied for orienting the single crystals prior to cutting them in specific crystallographic directions, for example, for the preparation of the wedge-shaped seed crystals. Due to the gentle cutting by the wire saw, as-sawn surfaces could be exposed to X-ray scattering without further treatment.

### 3.5.3. Electron-Probe Microanalysis

In order to determine the mole fraction  $x$  of the ternary  $\text{FeGa}_{3-x}\text{Ge}_x$  crystals, electron-probe microanalysis (EPMA) measurements were performed using a Cameca SX-100 system equipped with a  $\text{LaB}_6$  cathode and wavelength-dispersive (WDX) spectrometers. For EPMA analyses, slices with diamond-polished plane surfaces were fixed with electrically conductive silver lacquer. An accelerating voltage of 15 keV at a current of 40 nA was applied. Calibration was done using standards of binary  $\text{FeGa}_3$  and pure Ge.  $\text{Fe-K}_\alpha$  and  $\text{Ga-K}_\alpha$  lines were measured by the LiF detector and the TAP detector was used for  $\text{Ge-L}_\alpha$ .

### 3.5.4. Thermal Analysis

Differential thermal analysis (DTA) measurements were done in a Netzsch DTA (404/3/F) system under stationary Ar atmosphere of ambient pressure using open alumina crucibles (30  $\mu\text{L}$ ) and typically  $\approx 50$  mg samples.  $\text{Al}_2\text{O}_3$  powder was used as reference. The experiments were performed with heating and cooling rates of  $5\text{ K min}^{-1}$ . The DTA was calibrated using the melting point of Ge ( $T_m = 937.4^\circ\text{C}$ ) under identical conditions.

## 4. Results

### 4.1. Binary $\text{FeGa}_3$ Czochralski Experiments

Growing the very first  $\text{FeGa}_3$  Czochralski crystal had been the most challenging step since spontaneous nucleation was necessary and all trials to get the melt wetting the ceramic tip described above failed. When searching for the exact liquidus temperature which was done by thoroughly watching the melt surface during

slow cooling of the homogenized melt, we observed spontaneous nucleation of hundreds of tiny crystallites at the same time. Due to the tetragonal symmetry of  $\text{FeGa}_3$ , all crystallites were seen as tiny squares, that is, with their (001) faces parallel to the melt surface. Repeating this procedure very often, we never found only one or a few crystallites swimming at the surface. Moreover, trying to dissolve all but one of them by slow heating we failed as well. What was finally done was an unusual trick that succeeded only after repeating it several times. Using the tapered tip of the alumina rod that was fixed at the pulling rod, we trapped one of the crystallites swimming on the melt surface. Obviously, some rest of attached solution acted as a glue. Quick pulling removed the alumina tip with the crystal from the melt. After some overheating of the melt, all the competing crystallites were dissolved. Lowering the pulling rod toward the melt surface at conditions very close to the liquidus temperature brought the crystallite at the tip of the alumina rod again into contact with the melt and allowed to grow from this single seed. As mentioned above, this procedure succeeded only after several attempts. In most cases we lost the attached crystallite immediately after wetting the melt again.

The first crystal grown after applying this approach is pictured in **Figure 3a**. It was found to be not a single crystal but a two-grain ingot from the very beginning. Obviously, it had not been only a single crystallite that had been captured and served as the seed.

Nevertheless, one of the two grains was large enough to prepare a well-oriented [001] seed crystal for the first ordinary Czochralski growth experiment. The second crystal grown from a native seed can be seen in **Figure 3b**. It has been completely single-crystalline with the orientations of the seed, that is, pulled parallel to [001]. Several samples for further investigation were prepared from this crystal as well as a set of [001]-oriented seeds to be used for the next growth runs including those for  $\text{FeGa}_{3-x}\text{Ge}_x$  growth experiments.

### 4.2. $\text{FeGa}_{3-x}\text{Ge}_x$ Experiments

Ge-substituted  $\text{FeGa}_3$ , that is,  $\text{FeGa}_{3-x}\text{Ge}_x$  solid solutions were obtained from normal-freezing experiments in order to study the Ge segregation behavior. The starting charges as well as the obtained first-to-freeze compositions have been summarized in **Table 1**. Ge contents in these small ingots were measured by EPMA and are pictured versus the Ge composition in the starting solution in **Figure 4**.

The Czochralski growth experiments based upon the obtained knowledge on the Ge segregation behavior always resulted in single crystals. Single crystalline  $\text{FeGa}_{3-x}\text{Ge}_x$  ingots, all of them grown parallel [001], are shown in **Figure 5**. Special problems which had to be tackled during the growth process will be mentioned in the discussion section.

EPMA measurements on longitudinal (100) cut through the crystals revealed a weak but continuous increase in the Ge content (see **Figure 6**) which is well in accordance with the above mentioned segregations coefficient derived from **Figure 4**. Thus, for basic research on quantum criticality we were able to provide samples of fine-tuned Ge contents in the interesting composition range simply by preparing the pieces from the appropriate axial



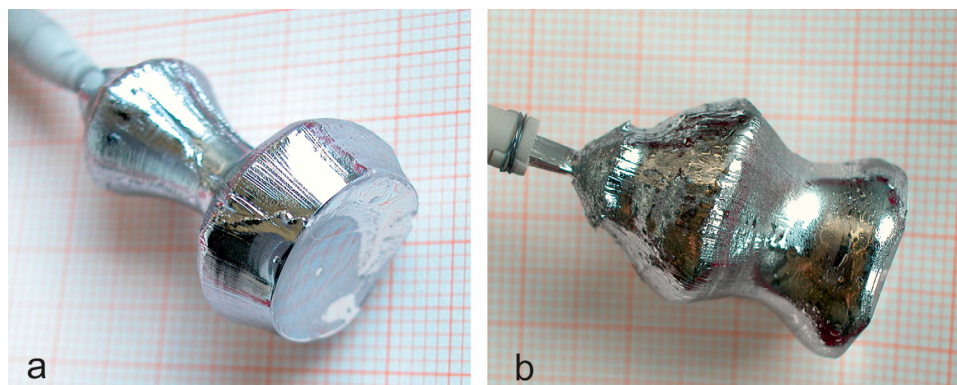


**Figure 3.** FeGa<sub>3</sub> crystals grown from Ga-rich solutions. While the very first crystal was obtained from spontaneous nucleation using a) a tapered alumina tip, b) the single crystal was grown using a [001]-oriented seed that is fixed in a seed holder shown in Figure 2.

**Table 1.** Overview on the pre-experiments with ternary samples to study the segregation behavior in order to qualify for the Czochralski growth runs. First-to-freeze compositions were measured by EPMA and normalized according to 25 at% Fe.

Starting charge		Experiment type	First-to-freeze
Melt composition	Total mass		
Fe <sub>16.0</sub> Ga <sub>82.6</sub> Ge <sub>1.4</sub>	11.3 g	Bridgman	FeGa <sub>2.95</sub> Ge <sub>0.05</sub>
Fe <sub>14.2</sub> Ga <sub>82.9</sub> Ge <sub>2.9</sub>	11.4 g	Bridgman	FeGa <sub>2.90</sub> Ge <sub>0.10</sub>
Fe <sub>14.0</sub> Ga <sub>81.7</sub> Ge <sub>4.3</sub>	11.5 g	Bridgman	FeGa <sub>2.85</sub> Ge <sub>0.15</sub>
Fe <sub>14.0</sub> Ga <sub>80.3</sub> Ge <sub>5.7</sub>	11.7 g	Bridgman	FeGa <sub>2.80</sub> Ge <sub>0.20</sub>
Fe <sub>13.6</sub> Ga <sub>79.2</sub> Ge <sub>7.2</sub>	11.8 g	Bridgman	FeGa <sub>2.78</sub> Ge <sub>0.22</sub>
Fe <sub>12.0</sub> Ga <sub>73.3</sub> Ge <sub>14.7</sub>	12.8 g	Bridgman	FeGa <sub>2.66</sub> Ge <sub>0.34</sub>
Fe <sub>14.33</sub> Ga <sub>83.65</sub> Ge <sub>2.02</sub>	47.2 g	Czochralski	FeGa <sub>2.95</sub> Ge <sub>0.05</sub>
Fe <sub>14.00</sub> Ga <sub>81.70</sub> Ge <sub>4.30</sub>	47.0 g	Czochralski	FeGa <sub>2.88</sub> Ge <sub>0.12</sub>
Fe <sub>13.90</sub> Ga <sub>81.15</sub> Ge <sub>4.95</sub>	45.6 g	Czochralski	FeGa <sub>2.87</sub> Ge <sub>0.13</sub>

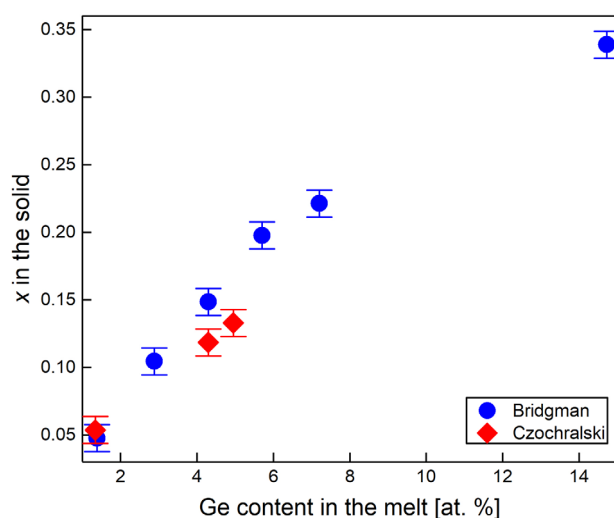


**Figure 4.** First-to-freeze composition  $x$  of FeGa<sub>3-x</sub>Ge<sub>x</sub> versus Ge content of the starting melt.

position within the crystal. The first-to-freeze compositions of the Czochralski-grown FeGa<sub>3-x</sub>Ge<sub>x</sub> crystals are included in Table 1.

**Figure 7** shows the result of a typical X-ray powder diffraction measurement of Ge-substituted FeGa<sub>3</sub> indicating phase-pure FeGa<sub>3-x</sub>Ge<sub>x</sub> material. Based on these Rietveld-refined powder diffraction diagrams, lattice parameters of various FeGa<sub>3-x</sub>Ge<sub>x</sub> samples were determined. Lattice parameter variations resulting from different Ge contents in the grown crystals can be seen from **Figure 8**. The small increase of the lattice parameter  $a$  with increasing Ge substitution  $x$  is accompanied by a stronger decreasing  $c$  lattice parameter resulting in a unit cell volume which becomes smaller by partly substituting Ge for Ga.

The peritectic decomposition temperatures of binary FeGa<sub>3</sub> and FeGa<sub>3-x</sub>Ge<sub>x</sub> measured by differential thermal analysis (DTA) are shown in **Figure 9**. For the undoped sample the signal of the cooling curve is pictured as well.

## 5. Discussion

After having succeeded with the abovementioned spontaneous nucleation procedure and the following seed selection which was done only in the very first experiment, the most challenging step in *all* Czochralski experiments was the formation of the shoulder region, that is, to slowly increase the crystal's diameter. The self-constructed Czochralski apparatus is not equipped with an automatic diameter control, and to the best of authors' knowledge, no crystal weighing system would be able to resolve the mass increase of the crystal resulting from growth rates as low as 25–50  $\mu\text{m h}^{-1}$ . This is the reason why diameter control was only done by slow temperature–time programs based on visual observation. Discussing the thermal conditions of the growing crystal, one should distinguish between the actual temperature at the growth interface which determines the diameter of the next layers to crystallize and the temperature indicated by the thermocouple close to the heater. Of course, there is always some difference between these temperatures, but during growing the shoulder the more effective radiation loss via the increasing diameter of the crystal results in additional cooling of the growth interface and, thus, speeds up crystallization even at a nominally unchanged temperature set point.

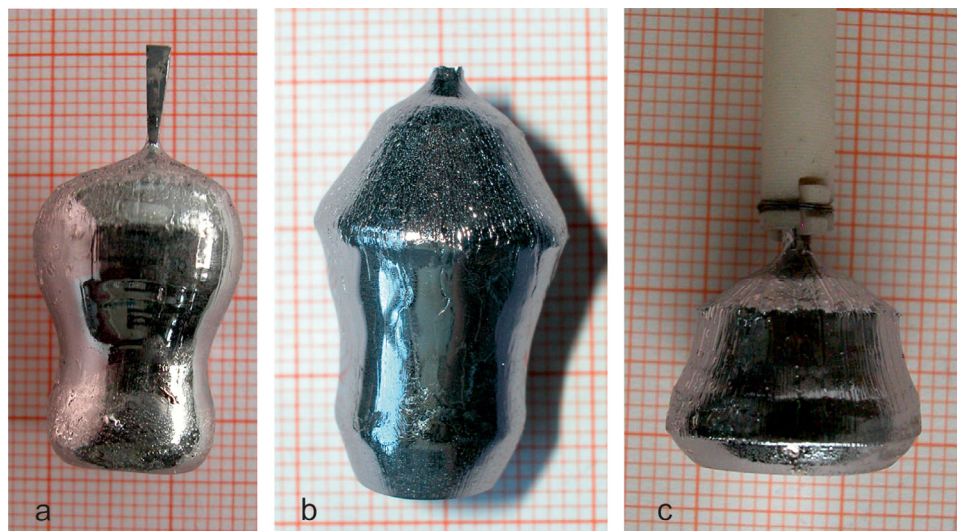


**Figure 5.** Czochralski-grown single crystals of  $\text{FeGa}_{3-x}\text{Ge}_x$  with different Ge contents  $x$  that are plotted in axial direction in Figure 6: average mole fraction a)  $x \approx 0.13$ , b)  $x \approx 0.15$ , and c)  $x \approx 0.06$ . All  $\text{FeGa}_{3-x}\text{Ge}_x$  Czochralski crystals of this study were grown from [001]-oriented  $\text{FeGa}_3$  seed crystals.

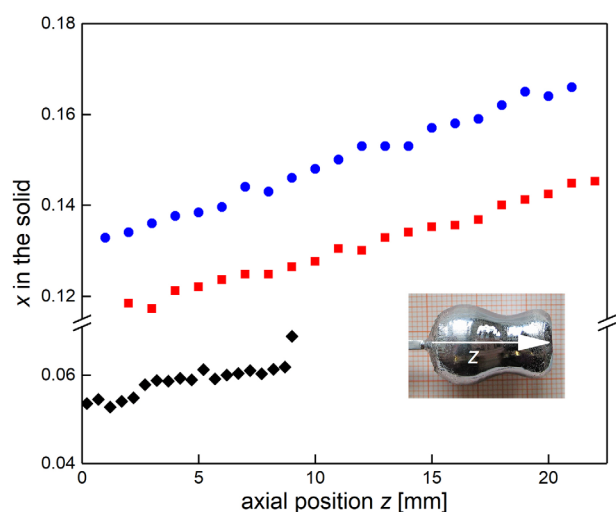


**Figure 6.** Axial Ge distribution  $x$  in  $\text{FeGa}_{3-x}\text{Ge}_x$  measured by EPMA on longitudinal sections through the single crystals. Systematic error bars are in the range of  $\Delta x = \pm 0.01$ .

Stable crystal growth always needs a limiting factor which may be the latent-heat release when using high enough pulling rates or the rejected excess component in solution growth experiments which reduces the liquidus temperature and, this way, limits further growth. Unfortunately, growing  $\text{FeGa}_3$  and related phases none of these limiting factors work effectively. Since the pulling rate has to be extremely low in order to avoid liquid inclusion formation, latent-heat release is a negligible quantity. Rejected Ga at the interface neither acts as a limiting factor due to the unusual slope of the liquidus curve being almost horizontal below the peritectic temperature (see Figure 1).

Even with a nominally constant heat supply, that is, with a constant set point of the temperature controller, radial crystal growth occurred in an uncontrolled manner and could only be stopped by positive temperature–time programs compensating

the additional loss of heat in this stage of the experiments. After having reached the intended final diameter of the crystals, their shapes were determined by the abovementioned programs to continuously decrease the temperature of the set point in order to compensate the compositional change of the remaining solution which is a complex function of the total amount of the starting melt, the present diameter of the crystal, and the phase diagram's liquidus. From the individual shapes of the single crystals pictured in Figures 3 and 5 it can be seen that this correction hardly succeeded in an ideal manner which is not a matter of concern if the grown crystals are later on cut into samples for basic research.

Although still not knowing the ternary Fe–Ga–Ge phase diagram, all crystal growth experiments done in this study can be used to determine a Ge segregation coefficient. The compositions given in the above sections have been expressed in at.% of the constituting components to describe the concentration of the starting melt and as Ge content  $x$  according to the general formula  $\text{FeGa}_{3-x}\text{Ge}_x$  in the solid phase. In order to define a segregation coefficient describing the change of the Ge content which occurs during crystallization, pseudobinary mole fractions,  $x_L$  and  $x_S$ , of the liquid ( $L$ ) and solid ( $S$ ) phases seem to be better suited, having in mind that Ge substitutes for Ga. Thus, the pseudobinary mole fraction is the ratio of  $N_{\text{Ge}}/(N_{\text{Ga}} + N_{\text{Ge}})$  with  $N_{\text{Ga}}$  and  $N_{\text{Ge}}$  being the number of the moles of the indicated components. With the data given in Table 1 which have been pictured in Figure 4, we get a segregation coefficient  $x_S/x_L \approx 1$  for all except the highest Ge contents of the Bridgman-type pre-experiments but  $x_S/x_L \approx 0.8$  for the three Czochralski-grown single crystals. The latter result is well in accordance with the slightly increasing Ge concentrations shown in the axial profiles of Figure 6, whereas the missing segregation obtained from the first-to-freeze analyses in the pre-experiments may result from fast crystallization after supercooling the melt.

Differential thermal analysis results (see Figure 9) indicate a slight decrease of the temperature of peritectic decomposition upon heating when  $\text{FeGa}_{3-x}\text{Ge}_x$  is compared with the binary

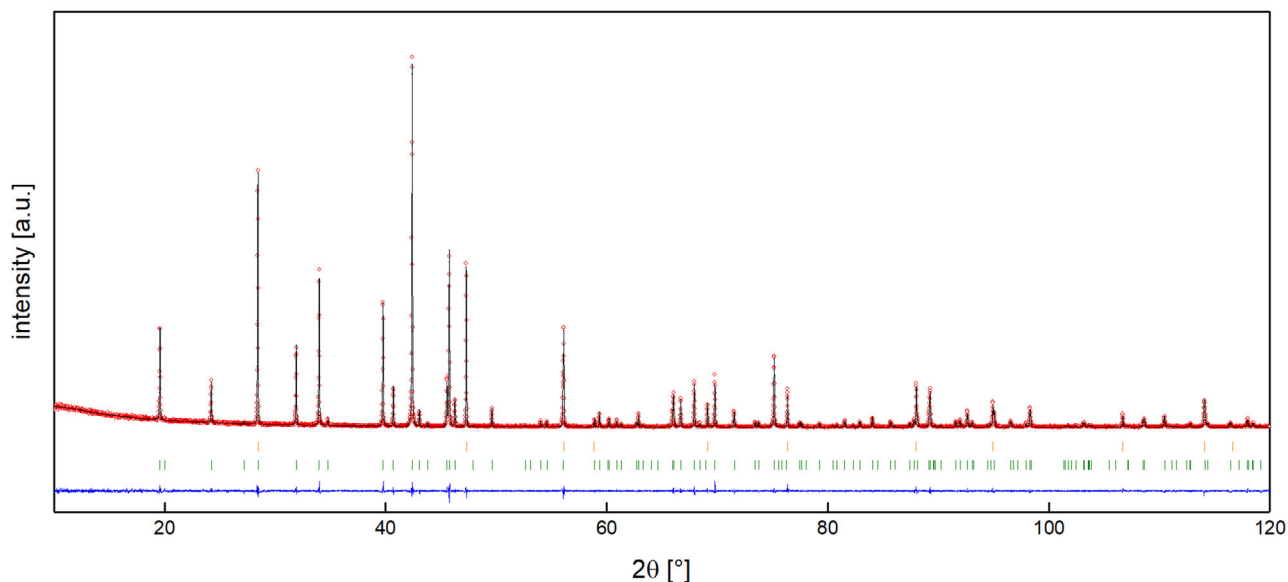


**Figure 7.** Observed (red circles), calculated (black line), and difference (blue line at the bottom) X-ray powder diffraction patterns of  $\text{FeGa}_{3-x}\text{Ge}_x$  ( $x = 0.12$ ) measured with  $\text{Cu-K}\alpha_1$  radiation. Green and orange tick marks indicate Bragg positions for the Ge-doped  $\text{FeGa}_3$  phase and Si 640c internal standard, respectively.

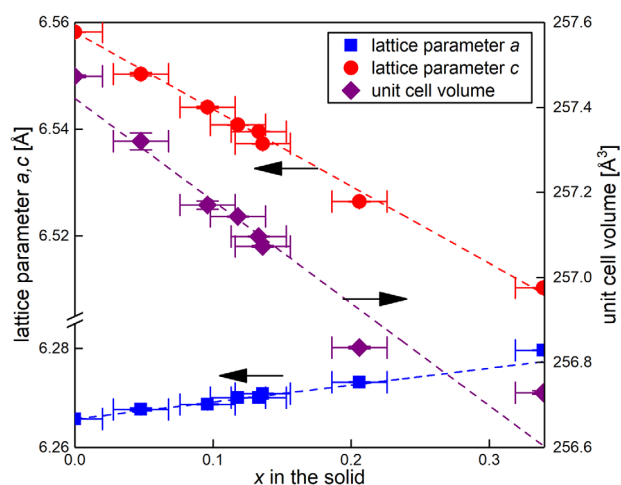


**Figure 8.** Unit cell parameter variations with increasing Ge content  $x$  of  $\text{FeGa}_{3-x}\text{Ge}_x$ .

$\text{FeGa}_3$ . Within the accuracy of the DTA apparatus, the  $\text{FeGa}_3$  peritectic temperature of 826 °C nicely agrees with the phase diagram data given by Okamoto.<sup>[22]</sup> DTA cooling curves with samples from intermetallic systems are usually less informative for two reasons: i) highly pure metallic melts show often huge undercooling and hardly allow to determine liquidus temperatures, and ii) with incongruent melting phases, once having completely molten the sample, the crystallization path of the homogenized melt is different from what occurred on heating. Nevertheless, what can be interpreted from the cooling curve in Figure 9 and from the Fe–Ga phase diagram (Figure 1) is that the onset of crystallization of  $\text{Fe}_3\text{Ga}_4$  from a melt of 75 at% Ga only occurred at 825 °C, immediately followed by  $\text{FeGa}_3$  formation.

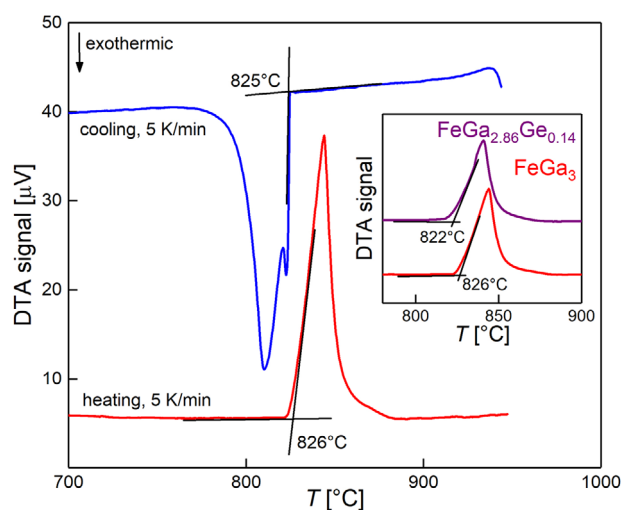


**Figure 9.** Differential thermal analysis of a binary  $\text{FeGa}_3$  sample compared to a Ge-doped one.

Based on the crystal growth results presented here, first measurements of physical properties of binary  $\text{FeGa}_3$  and  $\text{FeGa}_{3-x}\text{Ge}_x$  have already been published without mentioning details of the single crystal growth approach.<sup>[6,18,28]</sup> It is outside the scope of the present paper to repeat the results of the physical studies here.

## 6. Conclusion

$\text{FeGa}_3$  and  $\text{FeGa}_{3-x}\text{Ge}_x$  single crystal can be grown from Ga-rich solutions using the Czochralski method. [001]-oriented native seeds allowed the reproducible preparation of samples as large as a few  $\text{cm}^3$ . Single crystals free from solvent inclusions were

obtained by performing crystal growth at extremely low pulling rates down to  $25 \mu\text{m h}^{-1}$ . When partly substituting Ge for Ga, the axial Ge distribution in  $\text{FeGa}_{3-x}\text{Ge}_x$  reveals a pseudobinary segregation coefficient slightly lower than unity which leads to a weak increase in the Ge concentration along the growth direction.

## Acknowledgements

The authors are grateful to Yuri Grin, Michael Baenitz, and Jörg Sichelschmidt, all from Max-Planck-Institut für Chemische Physik fester Stoffe, Dresden, for initiating this project and for fruitful discussions. This work has been partly conducted within the European integrated Center for the development of new Metallic Alloys and Compounds (European C-MetAC).

## Conflict of Interest

The authors declare no conflict of interest.

## Keywords

Czochralski method, intermetallic semiconductors, solution growth, thermoelectrics

Received: April 23, 2019

Revised: September 2, 2019

Published online: September 16, 2019

- [1] U. Häussermann, M. Moström, P. Viklund, Ö. Rapp, T. Björnängen, *J. Solid State Chem.* **2002**, 165, 94.
- [2] R. Pöttgen, R.-D. Hoffmann, G. Kotzyba, *Z. Anorg. Allg. Chem.* **1998**, 624, 244.
- [3] N. Haldolaarachchige, W. A. Phelan, Y. M. Xiong, R. Jin, J. Y. Chan, S. Stadler, D. P. Young, *J. Appl. Phys.* **2013**, 113, 083709.
- [4] C. S. Lue, W. J. Lai, Y.-K. Kuo, *J. Alloys Compd.* **2005**, 392, 72.
- [5] Y. Hadano, S. Narazu, M. A. Avila, T. Onimaru, T. Takabatake, *J. Phys. Soc. Jpn.* **2009**, 78, 013702.
- [6] M. Wagner-Reetz, D. Kasinathan, W. Schnelle, R. Cardoso-Gil, H. Rosner, Y. Grin, P. Gille, *Phys. Rev. B* **2014**, 90, 195206.
- [7] E. M. Bittar, C. Capan, G. Seyfarth, P. G. Pagliuso, Z. Fisk, *J. Phys.: Conf. Ser.* **2010**, 200, 012014.
- [8] V. Yu. Verchenko, M. S. Likhanov, M. A. Kirsanova, A. A. Gippius, A. V. Tkachev, N. E. Gervits, A. V. Galeeva, N. Büttgen, W. Krätschmer, C. S. Lue, K. S. Okhotnikov, A. V. Shevelkov, *J. Solid State Chem.* **2012**, 194, 361.
- [9] K. Umeo, Y. Hadano, S. Narazu, T. Onimaru, M. A. Avila, T. Takabatake, *Phys. Rev. B* **2012**, 86, 144421.
- [10] B. Ramachandran, K. Z. Syu, Y. K. Kuo, A. A. Gippius, A. V. Shevelkov, V. Yu. Verchenko, C. S. Lue, *J. Alloys Compd.* **2014**, 608, 229.
- [11] M. Wagner-Reetz, R. Cardoso-Gil, Yu. Grin, *J. Electron. Mater.* **2014**, 43, 1857.
- [12] M. Cabrera-Baez, E. T. Magnavita, R. A. Ribeiro, M. A. Avila, *J. Electron. Mater.* **2014**, 43, 1988.
- [13] Y. Takagiwa, Y. Matsuura, K. Kimura, *J. Electron. Mater.* **2014**, 43, 2206.
- [14] A. A. Gippius, V. Yu. Verchenko, A. V. Tkachev, N. E. Gervits, C. S. Lue, A. A. Tsirlin, N. Büttgen, W. Krätschmer, M. Baenitz, M. Shatruk, A. V. Shevelkov, *Phys. Rev. B* **2014**, 89, 104426.
- [15] M. B. Gamza, J. M. Tomczak, C. Brown, A. Puri, G. Kotliar, M. C. Aronson, *Phys. Rev. B* **2014**, 89, 195102.
- [16] V. Ponnambalam, D. T. Morelli, *J. Appl. Phys.* **2015**, 118, 245101.
- [17] M. S. Likhanov, V. Y. Verchenko, M. A. Bykov, A. A. Tsirlin, A. A. Gippius, D. Bethebaud, A. Maignan, A. V. Shevelkov, *J. Solid State Chem.* **2016**, 236, 166.
- [18] B. Koo, K. Bader, U. Burkhardt, M. Baenitz, P. Gille, J. Sichelschmidt, *J. Phys.: Condens. Matter* **2018**, 30, 045601.
- [19] M. Majumder, M. Wagner-Reetz, R. Cardoso-Gil, P. Gille, F. Steglich, Y. Grin, M. Baenitz, *Phys. Rev. B* **2016**, 93, 064410.
- [20] a) Z. Fisk, J. P. Remieka, in *Handbook on the Physics and Chemistry of Rare Earths*, Vol. 12 (Eds: K. A. Gschneidner, Jr., L. Eyring), Elsevier, Amsterdam **1989**, Ch. 81; b) P. C. Canfield, Z. Fisk, *Philos. Mag. B* **1992**, 65, 1117.
- [21] P. F. S. Rosa, Z. Fisk, in *Crystal Growth of Intermetallics* (Eds: P. Gille, Yu. Grin), Walter de Gruyter, Berlin/Boston **2019**, Ch. 3.
- [22] H. Okamoto, *J. Phase Equilib. Diffus.* **2004**, 25, 100.
- [23] P. Gille, B. Bauer, *Cryst. Res. Technol.* **2008**, 43, 1161.
- [24] M. Hahne, P. Gille, *J. Cryst. Growth* **2014**, 401, 622.
- [25] P. Gille, in *Crystal Growth of Intermetallics* (Eds: P. Gille, Yu. Grin), Walter de Gruyter, Berlin/Boston **2019**, Ch. 4.
- [26] H. J. Scheel, *J. Cryst. Growth* **1972**, 13-14, 560.
- [27] J. Rodríguez-Carvajal, *Physica B* **1993**, 192, 55.
- [28] F. Wagner, R. Cardoso-Gil, B. Boucher, M. Wagner-Reetz, J. Sichelschmidt, P. Gille, M. Baenitz, Y. Grin, *Inorg. Chem.* **2018**, 57, 12908.